Journal of *Marine Science and Engineering*

MDPI

Article

Development of Initial Scantling Formulas for Submarine Deep Frames Based on Numerical Analysis

Minwoo Lee [1] and Dohan Oh [2,*]

[1] Naval Ship Design Department, Hanwha Ocean, 3370 Geoje-daero, Geoje-si 53302, Republic of Korea; minwoo24@hanwha.com
[2] Department of Naval Architecture and Ocean Engineering, Hongik University, Sejong 30016, Republic of Korea
* Correspondence: dohanoh@hongik.ac.kr; Tel.: +82-44-860-2582

Abstract

Submarine structures are typically classified into pressure hulls and non-pressure hulls. The pressure hull is a critical component designed to withstand external pressure at operational depths while ensuring internal structural integrity. It is generally composed of ring frames and bulkheads. However, in modern large-scale submarines, bulkheads are often replaced with deep frames to improve equipment layout flexibility. Deep frames serve as essential structural reinforcements, compensating for the loss of stiffness due to the absence of bulkheads. Despite their importance, research on the design of deep frames remains scarce, and in the absence of established design standards, engineers rely on conservative approaches based on practical experience. Therefore, the objective of this study is to propose initial scantling formulas for deep frames in submarine pressure hulls based on finite element analysis (FEA) and parametric studies. To this end, six design cases reflecting actual ship design ranges were selected, and the structural integrity of the pressure hull ring frames was verified through material and geometric nonlinear analysis using ANSYS Mechanical APDL. Subsequently, a total of 82,440 parametric studies were conducted with the reinforced shell thickness, effective length, height and thickness of the deep frame web, and the width and thickness of the deep frame flange as variables. As a result, the proposed formulas satisfied all Validation cases in terms of structural integrity and were found to be applicable within the section length range of 1.5 to 2.0 times the pressure hull diameter. The results of this study are expected to be effectively utilized in the initial design of deep frames for submarine pressure hulls.

Keywords: submarine; pressure hull; deep frame; buckling pressure; initial scantling; nonlinear finite element analysis

Check for updates

Academic Editor: Joško Parunov

Received: 18 January 2026
Revised: 13 February 2026
Accepted: 14 February 2026
Published: 18 February 2026

Copyright: © 2026 by the authors. Licensee MDPI, Basel, Switzerland. This article is an open access article distributed under the terms and conditions of the Creative Commons Attribution (CC BY) license.

1. Introduction

Submarines are essential naval weapon systems capable of conducting covert operations in deep waters, performing various missions such as anti-surface warfare, anti-submarine warfare, reconnaissance, and maritime surveillance. As shown in Figure 1, the hull structure of a submarine is categorized into the pressure hull, which resists external hydrostatic pressure while maintaining atmospheric conditions inside, and the non-pressure hull, which is not subjected to external pressure. Among them, the pressure hull is the most critical structural component, responsible for ensuring the safety of both crew and onboard equipment. It must maintain structural integrity under extreme conditions and withstand

the high pressures encountered at depths. Although a spherical shape offers the most stable form for a pressure hull, a cylindrical structure reinforced with ring frames is generally adopted due to its superior spatial efficiency and favorable hydrodynamic characteristics. Ring frames, typically of T-section and installed on the interior side of the shell, serve to reinforce the plating and prevent buckling. Bulkheads, which support the pressure hull and divide the internal compartments, are usually placed at regular intervals. However, in modern large submarines, the installation of bulkheads is often restricted due to design constraints and the need for optimal internal space utilization. In such cases, deep frames are employed to compensate for the loss of stiffness caused by the absence of bulkheads. Deep frames are arranged at intervals of approximately 1.5 to 2 times the diameter of the pressure hull to prevent the simultaneous buckling of the ring frames and shell plating. Compared to ring frames, they possess greater stiffness and size and are required to exhibit structural rigidity comparable to that of bulkheads.

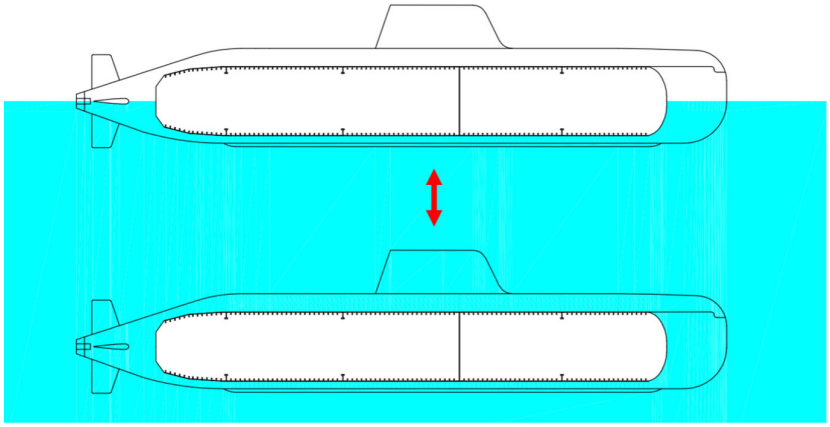


Figure 1. Pressure hull and Non-Pressure hull of Submarine indicates the submerged condition.

Since the 1920s, numerous studies have been conducted, primarily by the David Taylor Model Basin (DTMB), to establish empirical formulas for the design of submarine pressure hulls. Von Sander and Gunther investigated the theoretical stress distribution in shell plating supported by ring frames [1], and Faulkner subsequently proposed a corrected formulation to address errors identified in the original von Sander and Günther equations [2]. Lunchick also conducted a study focusing on shell yielding behavior under external pressure, contributing to the understanding of axisymmetric buckling [3]. Early investigations into shell buckling (asymmetric buckling) pressures of shell plating were carried out by Bryan and von Mises [4,5], while Windenburg and Trilling presented a simplified form of von Mises' formulation [6]. Studies on overall or general instability were conducted by Bryant and Kendrick [7,8]. Van der Neut investigated the buckling behavior of bulkhead-end plates and Ross later compiled theoretical analyses and experimental results on the collapse behavior of externally pressurized cylindrical, conical, and domed shells [9,10]. Based on these studies, several advanced countries have developed structural strength criteria applicable to their domestic submarine design and construction processes by systematically analyzing pressure hull collapse behavior. However, detailed and practical design information for pressure hulls remains limited. While considerable research has been conducted on shell plate thickness and ring frame spacing during the initial design phase, there is a relative lack of research on the primary structural elements of ring frames, namely the web and flange.

In recent years, numerous studies have been conducted to improve the structural efficiency of submarine pressure hulls. Oh and Koo proposed empirical formulas for the preliminary estimation of main dimensional parameters of ring-stiffened pressure hulls,

including shell thickness, frame spacing, web height and thickness, and flange width and thickness [11]. These formulas offer valuable guidance during the initial design stage. Kine investigated the influence of frame space and shell thickness on the buckling behavior of pressure hulls [12]. Rathinam et al. performed a comparative study between numerical and experimental buckling results, demonstrating the significant impact of initial geometric imperfections on buckling strength [13]. Şenol proposed a structural optimization method for pressure hulls, aiming at minimum weight and maximum internal volume [14]. Shinoka and Netto compared the efficiency of three metaheuristic algorithms: differential evolution (DE), particle swarm (PS), and simulated annealing (SA) for minimizing the structural weight of submarine pressure hulls [15]. Moreover, Burak Eyiler et al. studied the optimum structure of pressure hulls reinforced with various types of stiffeners [16]. However, these studies are all limited to ring frame structures, and studies on deep frames are difficult to find.

Deep frames, which possess significantly larger cross-sectional areas and higher stiffness than ring frames, play a critical role in supporting the pressure hull in place of bulkheads. Nevertheless, there are currently no clearly defined design standards or empirical formulas for deep frames, and publicly available data is scarce. Although some guidance suggests that deep frames should be designed with approximately three times the cross-sectional area and ten times the moment of inertia compared to ring frames, no standardized formulas or design methodologies based on this guidance have been established [17]. Moreover, DNV presents various analysis criteria and Validation procedures to ensure the structural safety of deep frames. However, these provisions merely require the designer to demonstrate the structural integrity of deep frames, and they do not offer empirical formulas or practical design guidelines for direct application in engineering practice [18].

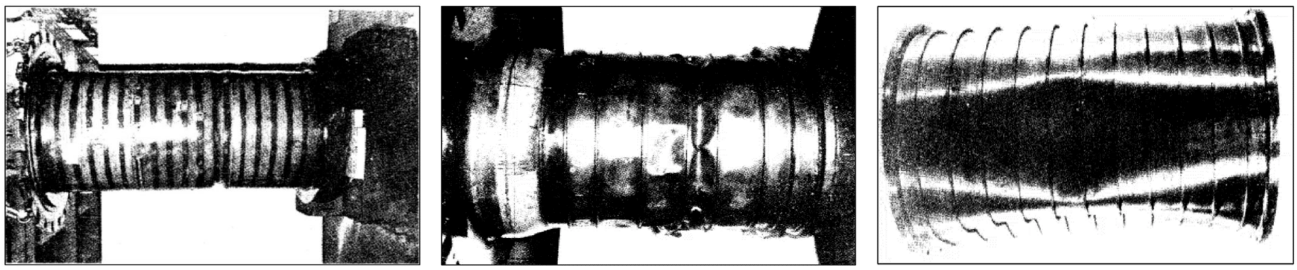
In this study, six design cases with different design pressures and pressure hull diameters were selected to derive the initial scantling formulas for the design of deep frames in submarine pressure hulls. The principal dimensions of the ring frames in each case were determined based on the estimation formulas proposed by Oh and Koo [11]. Structural integrity was verified using nonlinear buckling analysis through finite element analysis (FEA) and analytical calculations based on DNV [18]. Subsequently, a total of 82,440 parametric studies were conducted using FEA, in which the design variables included the section length (L_{sec}) of the pressure hull, the reinforced shell thickness, the effective length of the deep frame, and the web height and thickness, as well as the flange width and thickness of the deep frames. The FEA was performed using the general-purpose software ANSYS Mechanical APDL 2024 R2, and both linear buckling analysis and nonlinear buckling analysis incorporating material and geometric nonlinearities were conducted. Based on the results, initial scantling formulas for the principal dimensions of deep frame members are proposed.

2. Failure Modes of Submarine Pressure Hulls

The failure modes of submarine pressure hulls are highly complex due to the influence of various structural components. However, as the pressure hull is typically cylindrical to maximize internal space efficiency, it is highly vulnerable to buckling. Therefore, the most critical consideration in pressure hull design is failure due to buckling. A ring-frame-stiffened pressure hull must be designed to prevent elastic buckling, which can occur before the material reaches its yield stress, and the buckling strength must be greater than the hydrostatic pressure corresponding to the submarine's design depth.

Representative buckling modes of a ring-frame-stiffened pressure hull include shell yielding, shell buckling, and general instability. As shown in Figure 2a, shell yielding

occurs at the center of the shell between ring frames when the shell is relatively thick and the ring frame spacing is narrow. This type of failure exhibits axisymmetric accordion-like wrinkling. As shown in Figure 2b, shell buckling occurs between ring frames when the shell is relatively thin and the frame spacing is wide, resulting in small circumferential wrinkles along the shell. In Figure 2c, general instability occurs when both the shell and ring frames collapse simultaneously. This happens when the spacing between high-stiffness reinforcements or bulkheads is large, or when the strength of the ring frames is insufficient.



(**a**) (**b**) (**c**)

Figure 2. (**a**) Shell Yielding; (**b**) Shell Buckling; (**c**) General Instability [19].

3. Design Cases

3.1. Initial Dimensions of Ring Frames

In this study, six cases with different combinations of design pressure and pressure hull diameter were selected based on a survey of actual submarine design data, and the initial dimensions of the ring frames for each case were established. As shown in Figure 3, the ring frame dimensions include the shell thickness (t_s), frame space (L_{fs}), web height (h_w) and thickness (t_w), and flange width (b_f) and thickness (t_f). These values were calculated based on the estimation formulas proposed by Oh and Koo [11]. The corresponding data are presented in Tables 1 and 2.

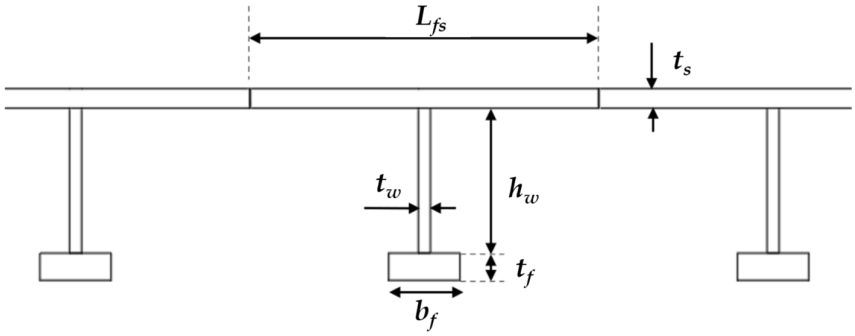


Figure 3. Section of Ring frame with Main Parameters.

The design pressure applied to a submarine pressure hull corresponds to the Collapse Diving Pressure (CDP), which is defined as the Nominal Diving Pressure (NDP) multiplied by a safety factor. The nominal diving depth (NDD) defines the maximum diving depth for unrestricted diving operations in seawater of the submarine [18]. In this study, the design pressures were determined based on a survey of existing submarines, using the safety factor specified by DNV [18], as described in Equation (1).

$$\mathrm{CDP/NDP} = 8/\mathrm{NDP} + 1.6\ (\mathrm{bar}) \quad (1)$$

Table 1. Case Data of Pressure hull.

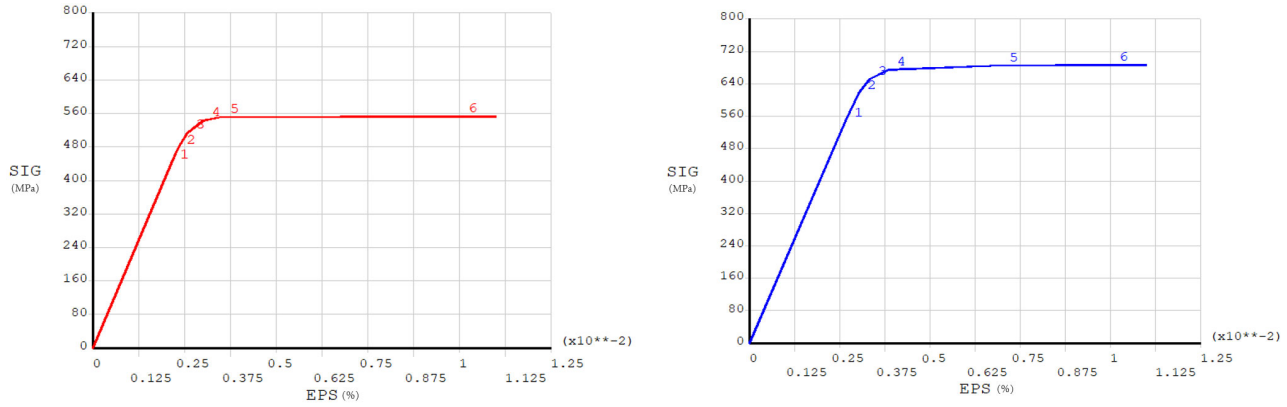
Case	Design Pressure (MPa)	Diameter (mm)	Ring Frame Material	Deep Frame Material
1	5.5	6200	HY80	HY80
2	6.0	7600	HY100	HY80
3	5.5	8000	HY80	HY80
4	6.0	9000	HY80	HY80
5	7.0	10,000	HY100	HY80
6	7.5	12,000	HY100	HY80

Table 2. Initial Dimensions of ring frame (mm).

Case	Shell Thickness (t_s)	Frame Space (L_{fs})	Web Height (h_w)	Web Thickness (t_w)	Flange Width (b_f)	Flange Thickness (t_f)
1	24.5	430	185	15.5	90	35.0
2	27.0	500	200	17.5	105	38.0
3	31.5	550	235	20.0	120	44.5
4	38.5	650	290	25.0	145	50.0
5	40.5	700	305	26.0	155	55.0
6	52.5	870	390	33.5	200	73.5

3.2. Material Properties

In submarine design, HY-80 steel is commonly used for the pressure hull, although HY-100 steel is sometimes applied to reduce structural weight. Therefore, in this study, HY-80 and HY-100 steels were applied as ring frame material. However, for deep frames, HY-80 steel was used in all cases due to its superior weldability and lower cost. The mechanical properties and yield strengths of both materials are presented in Table 3, as specified in MIL-S-16216K [20]. Finite element analysis was conducted using ANSYS Mechanical APDL. As shown in Figure 4, material nonlinearity was modeled by applying a multi-linear material model based on the stress–strain curve. The allowable stress in this curve was defined with reference to the yield strength of the material.



(**a**) (**b**)

Figure 4. (**a**) Stress–Strain Curve of HY80; (**b**) Stress–Strain Curve of HY100. (The symbol ** signifies scientific notation).

Table 3. Material Properties of HY80 and HY100.

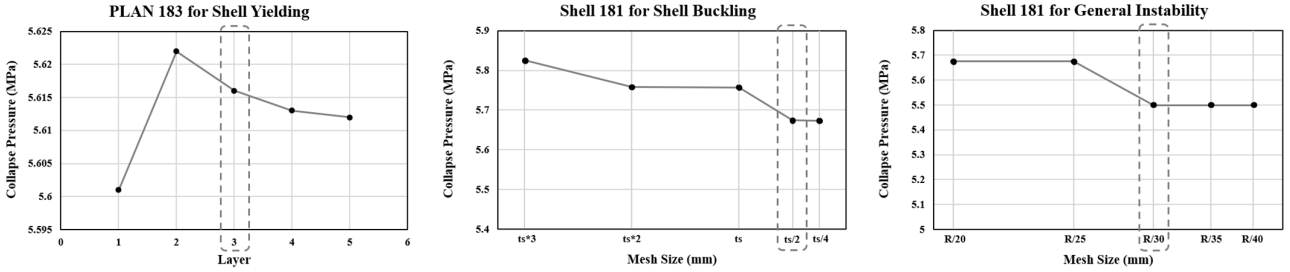
Property	HY80	HY100
Young's Modulus (MPa)	206,000	206,000
Poisson's Ratio	0.3	0.3

Table 3. *Cont.*

Property	HY80	HY100
Density (ρ) (g/mm^3)	7.85×10^{-3}	7.85×10^{-3}
Yield Strength (MPa)	552	686

3.3. Mesh Convergence Study for Finite Element Method

To ensure numerical accuracy and solution convergence, a mesh convergence study was carried out for the three analyses, namely shell yielding, shell buckling, and general instability. PLAN183 was used for shell yielding, and 3 layers through the thickness were selected in consideration of both convergence and computational efficiency. For shell buckling and general instability, SHELL181 was used with convergence achieved at mesh sizes of t/2 and R/30, respectively. These mesh configurations were applied throughout the parametric study. Convergence results are shown in Figure 5.



(**a**) (**b**) (**c**)

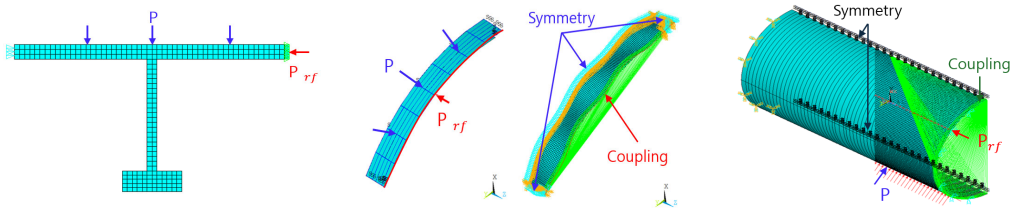
Figure 5. Mesh Convergence study results of the mesh size and collapse pressure for Finite Element Analysis: (**a**) for Shell Yielding; (**b**) for Shell Buckling; (**c**) for General Instability. (Dotted line represents the selected mesh size, and the symbol "*" indicates multiplication).

4. Structural Integrity Evaluation of Ring Frames

4.1. Boundary Conditions and Modeling for FEA

The buckling analysis was divided into three categories based on the intended failure mode: shell yielding, shell buckling, and general instability. For shell yielding analysis, the two-dimensional structural continuum element PLAN183 was used. This element enables axisymmetric characteristics to be activated in a 2D plane, allowing for results like those of 3D analysis. In contrast, SHELL181, a four-node element with six degrees of freedom, was used for shell buckling and general instability analysis. This element is suitable for both linear and nonlinear analysis involving large deformations.

In all buckling analyses, the shell plating was subjected to pressure higher than the design pressure. In addition, ring force and coupling loads were applied at the fore and aft ends in the axial direction. Boundary conditions were applied according to the characteristics of each buckling mode, as summarized in Table 4, and the corresponding modeling approaches are illustrated in Figure 6.



(**a**) (**b**) (**c**)

Figure 6. (**a**) FEA for Shell Yielding; (**b**) FEA for Shell Buckling; (**c**) FEA for General Instability.

The section length, defined as the spacing between bulkheads or deep frames in the pressure hull, is typically 1.5 to 2 times the diameter of the pressure hull. Therefore, in the general instability analysis, the section length was set to twice the pressure hull diameter, which is the maximum considered in this study.

Table 4. Boundary Condition for Buckling.

		Shell Yielding	Shell Buckling	General Instability
Element		**PLAN 183**	**SHELL 181**	**SHELL 181**
Boundary Condition	Constrain	Coupling and Fixed to longitudinal direction	Coupling and Symmetry	Coupling, Fixed all, Fixed to circumferential direction and Symmetry
	Loading	$P = \alpha \times P_{Design}$ and $P_{rf} = \frac{R_{out}^2}{R_{out}^2 - R_{in}^2} \times P$		

4.2. Buckling Analysis Results

From the shell yielding analysis incorporating initial imperfections, all design cases satisfied the design pressure. This confirms that the ring frame dimensions determined by the initial scantling formulas ensure structural stability against shell yielding. Furthermore, as shown in Table 5, the deviation between the analytically calculated buckling strength and the value estimated through finite element analysis was within 5.0%. This validates the accuracy of the numerical approach.

Table 5. Comparison of Shell Yielding Pressure by Analytic Method and Numerical Method.

Case	1	2	3	4	5	6
P_{cr}_*analytical* (MPa)	6.348	7.145	6.344	7.061	8.520	8.874
P_{cr}_*numerical* (MPa)	6.519	6.874	6.521	7.145	8.019	8.836
Difference (%)	2.7	3.8	2.8	1.2	5.0	0.4

Similarly, the shell buckling analysis with initial imperfections showed that all design cases satisfied the design pressure. Therefore, the ring frame dimensions based on the initial scantling formulas were also confirmed to be structurally stable against shell buckling. As presented in Table 6, the difference between the analytically and numerically obtained buckling strengths was within 5.8%.

Table 6. Comparison of Shell Buckling Pressure by Analytic Method and Numerical Method.

Case	1	2	3	4	5	6
P_{cr}_*analytical* (MPa)	6.607	6.419	6.690	7.667	8.094	8.776
P_{cr}_*numerical* (MPa)	6.671	6.739	6.542	7.220	8.064	8.743
Difference (%)	0.2	5.0	2.2	5.8	0.4	0.4

For the general instability analysis, an initial imperfection corresponding to 0.2% of the pressure hull diameter was applied. This value represents the maximum allowable out-of-roundness [12]. As shown in Table 7, the buckling strength of all design cases exceeded the design pressure under these conditions. This result confirms that the ring frame dimensions derived from the initial scantling formulas maintain structural integrity under general instability when the section length equals twice the pressure hull diameter. Therefore, within the section length range considered in this study (1.5 to 2.0 times the pressure hull diameter), the selected ring frame dimensions are considered appropriate.

Table 7. Comparison of Design Pressure and General Instability Pressure by Numerical.

Case	1	2	3	4	5	6
P_{Design} (MPa)	5.500	6.000	5.500	6.000	7.000	7.500
P_{cr} (MPa)	6.100	6.175	6.100	6.775	7.350	8.175
P_{cr}/P_{Design} Ratio	1.11	1.03	1.11	1.13	1.05	1.09

5. Parametric Study

5.1. Bounds and Discrete Value

A total of 82,440 parametric studies were conducted using finite element analysis for six design cases with different combinations of design pressure and pressure hull diameter. The design variables included the section length (L_{sec}), reinforced shell thickness (t_{rein}), effective length (L_{eff}), deep frame web height (h_{wd}) and thickness (t_{wd}), and deep frame flange width (b_{fd}) and thickness (t_{fd}). The overall geometry of the deep frame and the definition of each design variable are shown in Figure 7. The parametric bounds for each design variable were selected based on structural efficiency, under the assumption that deep frames function similarly to bulkheads. Among the parameters, t_{rein} and L_{eff} were applied with the same design range for all section lengths, as shown in Table 8. The remaining variables were defined with separate design ranges depending on the section length, as presented in Tables 9–14.

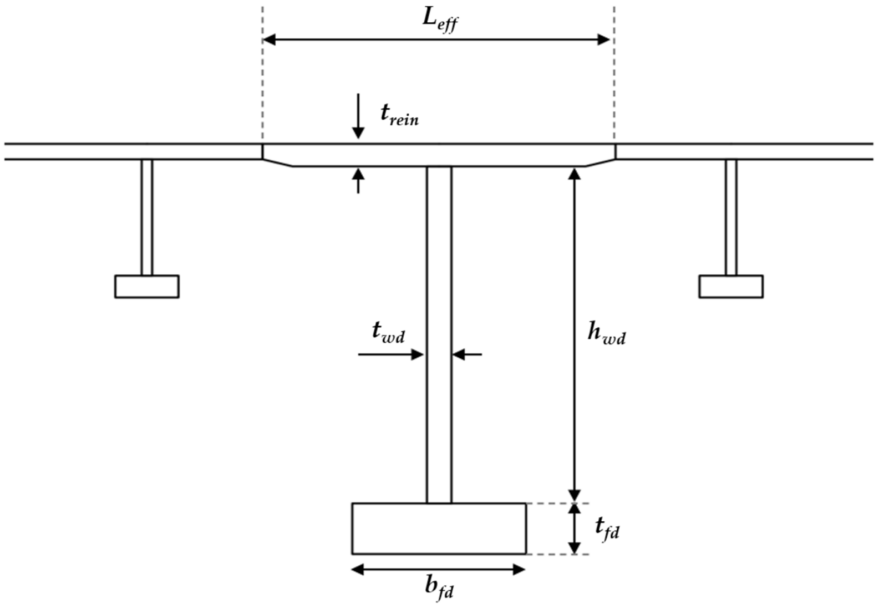


Figure 7. Section of Deep frame with Main Parameters.

Table 8. Bounds and Discrete values of t_{rein} and L_{eff} (mm).

Case		t_{rein}	L_{eff}
1	Bound	36.0~38.0	520~530
	Discrete value	0.5	5
2	Bound	46.5~48.5	650~670
	Discrete value	0.5	10
3	Bound	46.5~48.5	670~690
	Discrete value	0.5	10

Table 8. *Cont.*

Case		t_{rein}	L_{eff}
4	Bound Discrete value	57.0~59.0 0.5	780~800 10
5	Bound Discrete value	72.0~76.0 1	930~950 10
6	Bound Discrete value	95.0~99.0 1	1170~1190 10

Table 9. Bounds and Discrete values for Section length 1.5 D (mm).

Case		h_{wd}	t_{wd}	b_{fd}	t_{fd}
1	Bound Discrete value	465~480 5	25.0~26.0 0.5	225~235 5	65.5~68.5 1
2	Bound Discrete value	505~520 5	28.0~29.0 0.5	250~260 5	71.5~74.5 1
3	Bound Discrete value	590~605 5	31.5~33.5 1	300~310 5	76~78 1
4	Bound Discrete value	715~745 10	40.0~42.0 1	365~380 5	94~97 1
5	Bound Discrete value	745~775 10	41.5~43.5 1	375~390 5	104~107 1
6	Bound Discrete value	970~1000 10	53.0~56.0 1	500~520 10	133~136 1

Table 10. Bounds and Discrete values for Section length 1.6 D (mm).

Case		h_{wd}	t_{wd}	b_{fd}	t_{fd}
1	Bound Discrete value	485~500 5	26.0~27.0 0.5	235~245 5	68~71 1
2	Bound Discrete value	525~540 5	28.5~30.5 1	255~265 5	75~77 1
3	Bound Discrete value	615~635 10	33~35 1	310~320 5	78~81 1
4	Bound Discrete value	780~810 10	41.5~43.5 1	380~390 5	99~102 1
5	Bound Discrete value	770~800 10	42.5~44.5 1	385~395 5	106~109 1
6	Bound Discrete value	1000~1030 10	54.0~56.0 1	510~520 10	134~138 1

Table 11. Bounds and Discrete values for Section length 1.7 D (mm).

Case		h_{wd}	t_{wd}	b_{fd}	t_{fd}
1	Bound Discrete value	505~520 5	27.5~28.5 0.5	245~255 5	73~75 1
2	Bound Discrete value	560~575 5	31.0~32.5 0.5	275~285 5	79~81 1

Table 11. *Cont.*

	Case	h_{wd}	t_{wd}	b_{fd}	t_{fd}
3	Bound	655~670	35.0~37.0	330~340	83~86
	Discrete value	5	1	5	1
4	Bound	800~830	44.0~46.0	400~415	104~107
	Discrete value	10	1	5	1
5	Bound	835~865	45.5~47.5	410~425	115~117
	Discrete value	10	1	5	1
6	Bound	1075~1105	58.0~60.0	550~565	146~149
	Discrete value	10	1	5	1

Table 12. Bounds and Discrete values for Section length 1.8 D (mm).

	Case	h_{wd}	t_{wd}	b_{fd}	t_{fd}
1	Bound	525~540	28.5~29.5	255~265	75~76
	Discrete value	5	0.5	5	1
2	Bound	580~600	32.0~33.0	285~295	81~84
	Discrete value	5	0.5	5	1
3	Bound	680~700	36.5~37.5	345~355	86~89
	Discrete value	5	0.5	5	1
4	Bound	840~860	45.5~47.5	415~430	108~111
	Discrete value	5	1	5	1
5	Bound	870~900	47.5~49.5	425~440	118~121
	Discrete value	10	1	5	1
6	Bound	1115~1145	60.0~62.0	575~590	151~154
	Discrete value	10	1	5	1

Table 13. Bounds and Discrete values for Section length 1.9 D (mm).

	Case	h_{wd}	t_{wd}	b_{fd}	t_{fd}
1	Bound	560~575	30.5~31.5	275~285	80~83
	Discrete value	5	0.5	5	1
2	Bound	625~640	34.0~35.0	305~315	87~90
	Discrete value	5	0.5	5	1
3	Bound	725~740	38.5~40.5	365~375	92~95
	Discrete value	5	1	5	1
4	Bound	895~910	49.0~51.0	445~465	115~118
	Discrete value	5	1	5	1
5	Bound	935~950	51.0~53.0	460~475	127~129
	Discrete value	5	1	5	1
6	Bound	1200~1230	64.5~66.5	610~630	162~165
	Discrete value	10	1	5	1

Table 14. Bounds and Discrete values for Section length 2.0 D (mm).

	Case	h_{wd}	t_{wd}	b_{fd}	t_{fd}
1	Bound	590~605	31.5~32.5	290~305	85~86
	Discrete value	5	0.5	5	1
2	Bound	655~675	36.0~38.0	320~330	91~94
	Discrete value	5	1	5	1

Table 14. *Cont.*

Case		h_{wd}	t_{wd}	b_{fd}	t_{fd}
3	Bound	760~780	41.0~43.0	385~395	96~99
	Discrete value	5	1	5	1
4	Bound	950~965	51.0~53.0	465~475	121~123
	Discrete value	5	1	5	1
5	Bound	980~995	53.0~55.0	485~495	133~135
	Discrete value	5	1	5	1
6	Bound	1250~1280	67.5~69.5	640~655	170~173
	Discrete value	10	1	5	1

5.2. Constraints

The constraints applied in the parametric study include the allowable fatigue stress, the design pressure, and the general instability strength. As shown in Equation (2), the allowable fatigue stress of the material must not be less than the numerical fatigue stress of the structure. According to DNV, submarine pressure hulls are required to satisfy the allowable fatigue stress corresponding to 10,000 cycles at the nominal diving depth [18].

$$\sigma_{allowablefatiguestress} > \sigma_{numericalfatiguestress} \tag{2}$$

The design pressure must also be lower than the collapse strength of the structure, as indicated in Equation (3).

$$P_{cr} > P_{design} \tag{3}$$

For general instability strength, the critical load of the buckling mode in which the deep frame acts as a bulkhead must not be lower than the critical load of the mode in which the deep frame collapses together with the shell, as expressed in Equation (4).

$$P_{cr_bulkhead} > P_{cr_togerther} \tag{4}$$

5.3. Boundary Conditions and Modeling

The fatigue and structural strength analysis of the deep frames for the parametric study was performed using PLAN 183 elements. The boundary conditions and modeling approach are shown in Figure 8a and Table 15.

Table 15. Boundary Conditions for Parametric Study.

			Fatigue and Structural Strength		**Shell Buckling**	
Element			**PLAN 183**		**SHELL 181**	
Boundary Condition	Constrain		Coupling, Fixed all		Coupling, Fixed all, Fixed to circumferential direction and Symmetry	
	Loading	Linear	$P = P_{NDD}$	$P_{rf} = \frac{R_{out}^2}{R_{out}^2 - R_{in}^2} \times P$	$P = 1$ MPa	$P_{rf} = \frac{R_{out}^2}{R_{out}^2 - R_{in}^2} \times P$
		Nonlinear	$P = \alpha \times P_{Design}$		$P = \alpha \times P_{Design}$	

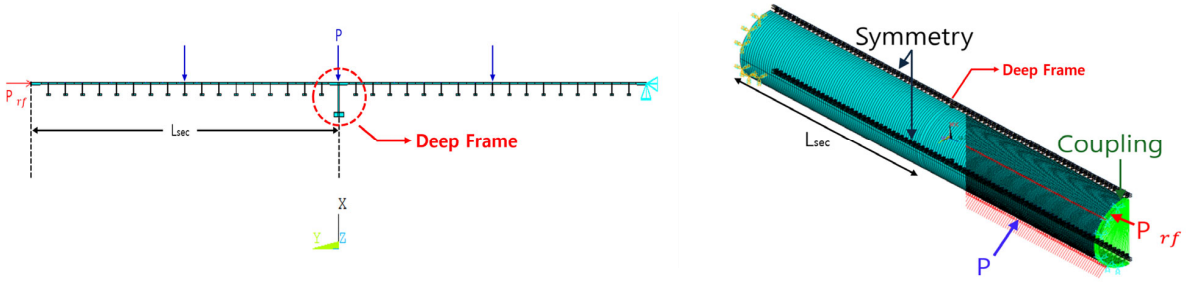
Fatigue strength analysis was carried out through linear analysis, where the nominal diving pressure (P_{NDD}) as shown in Table 16 was calculated using Equation (1) based on DNV [18]. Structural strength analysis was conducted through nonlinear analysis using the design pressure as the load condition.

The general instability strength analysis of the deep frames was modeled as shown in Figure 8b. For the linear buckling analysis, an external pressure of 1 MPa was applied to the

shell plating of the pressure hull. The analysis was repeated until the target buckling mode shape was obtained. And nonlinear analysis with initial imperfection was then performed to assess structural integrity.

Table 16. Nominal Diving Pressure for each design case (MPa).

Case	1	2	3	4	5	6
P_{NDD} (MPa)	3.00	3.25	3.00	3.25	3.88	4.19



(**a**) (**b**)

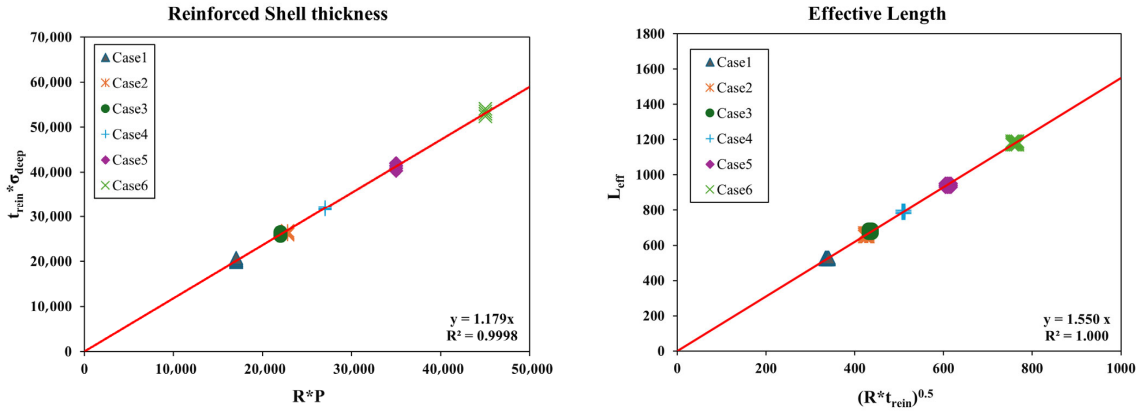
Figure 8. (**a**) FEA Model for Fatigue and Structural Strength of Deep frame; (**b**) FEA Model for General Instability of Deep frame. (The dotted line indicates the deep frame structure).

6. Initial Scantling Formulas for Submarine Deep Frames

Based on parametric study, initial scantling formulas for submarine deep frames were derived, as summarized in Table 17. These formulas were obtained using a curve fitting method, and the corresponding plots are shown in Figure 9a–f. σ_{ring} is the yield strength of the ring frame material, and σ_{deep} is that of the deep frame material.

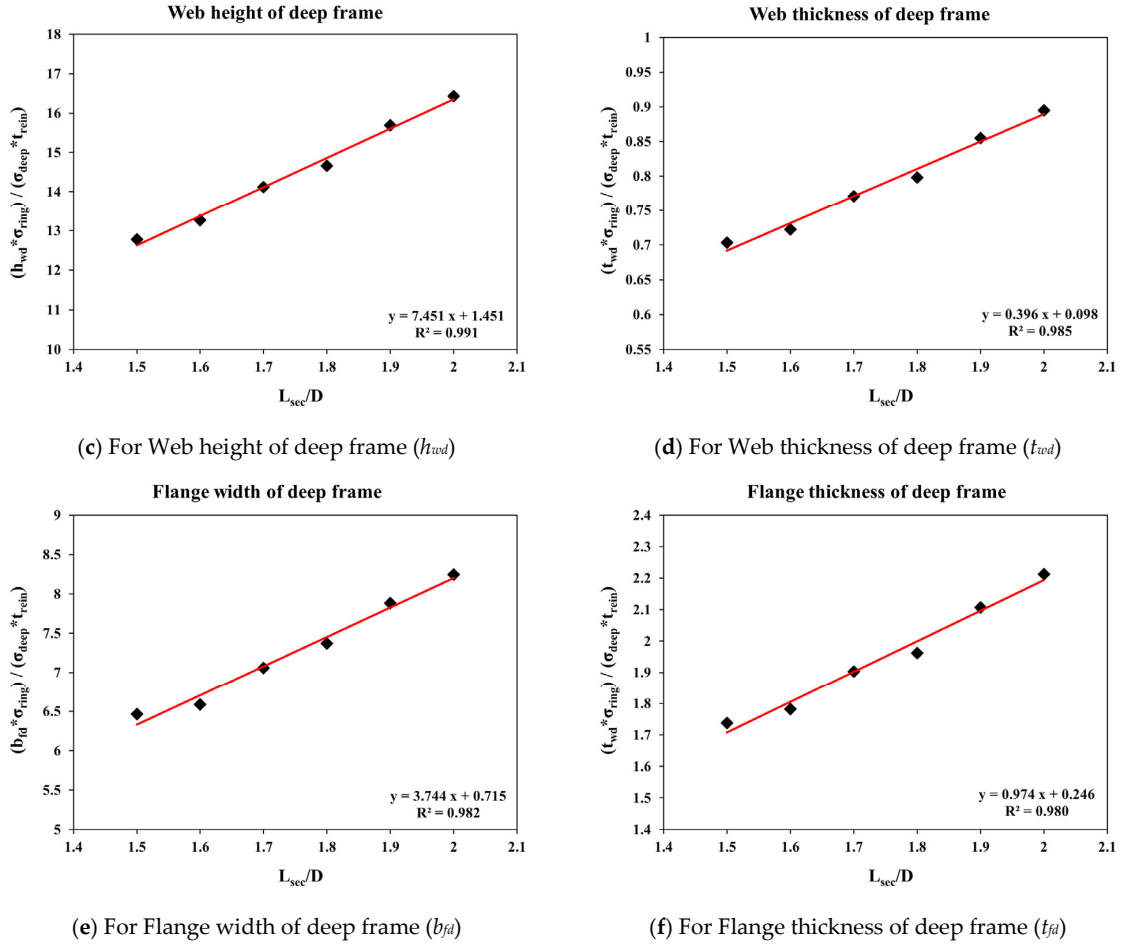
Table 17. Initial Scantling Formulas for Submarine Deep frames by Parametric Study.

Parameters	Initial Scantling Formulas	
Reinforced Shell Thickness (t_{rein})	$t_{rein} = 1.179 \times \frac{PR}{\sigma_{deep}}$	
Effective Length of Deep frame (L_{eff})	$L_{eff} = 1.550 \times \sqrt{R \cdot t_{rein}}$	
Web height of Deep frame (h_{wd})	$h_{wd} = \left(7.451 \times \frac{L_{sec}}{D} + 1.451\right) \times t_{rein} \times \frac{\sigma_{deep}}{\sigma_{ring}}$	$h_{wd} = \left(8.785 \times \frac{L_{sec}}{D} + 1.711\right) \times \frac{PR}{\sigma_{ring}}$
Web thickness of Deep frame (t_{wd})	$t_{\mathrm{wd}} = \left(0.396 \times \frac{L_{sec}}{D} + 0.098\right) \times t_{rein} \times \frac{\sigma_{deep}}{\sigma_{ring}}$	$t_{\mathrm{wd}} = \left(0.467 \times \frac{L_{sec}}{D} + 0.116\right) \times \frac{PR}{\sigma_{ring}}$
Flange height of Deep frame (b_{fd})	$b_{fd} = \left(3.744 \times \frac{L_{sec}}{D} + 0.715\right) \times t_{rein} \times \frac{\sigma_{deep}}{\sigma_{ring}}$	$b_{fd} = \left(4.414 \times \frac{L_{sec}}{D} + 0.843\right) \times \frac{PR}{\sigma_{ring}}$
Flange thickness of Deep frame (t_{fd})	$t_{fd} = \left(0.974 \times \frac{L_{sec}}{D} + 0.246\right) \times \mathrm{t_{rein}} \times \frac{\sigma_{deep}}{\sigma_{ring}}$	$t_{fd} = \left(1.148 \times \frac{L_{sec}}{D} + 0.290\right) \times \frac{PR}{\sigma_{ring}}$



(**a**) For Reinforced Shell thickness (t_{rein}) (**b**) For Effective length (L_{eff})

Figure 9. *Cont.*



(**c**) For Web height of deep frame (h_{wd})

(**d**) For Web thickness of deep frame (t_{wd})

(**e**) For Flange width of deep frame (b_{fd})

(**f**) For Flange thickness of deep frame (t_{fd})

Figure 9. Estimated Curves of Deep frame Parameters ("*" denotes multiplication).

7. Validation of the Initial Scantling Formulas for Deep Frames

7.1. Validation Cases

To validate the applicability of the initial scantling formulas proposed in this study, several Validation cases with different section lengths were evaluated. For each case, the deep frame dimensions were estimated using the derived formulas, and structural stability was assessed accordingly. The section lengths for the Validation cases were selected within the range of 1.5 to 2.0 times the pressure hull diameter, as shown in Table 18. The estimated deep frame dimensions obtained from the formulas are listed in Table 19. The boundary conditions and modeling for the FEA are identical to those presented in Figure 8 and Table 16.

Table 18. Section lengths by Case for Validation.

Case	L_{sec}	Case	L_{sec}
1	1.5 D	4	1.8 D
2	1.6 D	5	1.9 D
3	1.7 D	6	2.0 D

Table 19. Dimensions of Deep frame for Validation (mm).

Case	t_{rein}	L_{eff}	h_{wd}	t_{wd}	b_{fd}	t_{fd}
1	36.5	520	465	25.0	230	65
2	48.5	665	525	29.0	265	70

Table 19. *Cont.*

Case	t_{rein}	L_{eff}	h_{wd}	t_{wd}	b_{fd}	t_{fd}
3	47.0	670	665	36.5	335	90
4	57.5	790	860	47.0	430	115
5	75.0	950	940	52.0	475	125
6	96.0	1180	1260	70.0	635	170

7.2. Review Results

The fatigue strength analysis evaluated whether the stress occurring at the connection between the deep frame web and the reinforced shell plate was within the allowable fatigue stress. The allowable fatigue stress of HY-80 steel was reported to be 499.435 MPa by Oh and Ahn (2019) [21], and as shown in Table 20, all Validation cases satisfied the fatigue strength requirements. This confirms that the deep frames designed using the proposed initial scantling formulas are appropriate in terms of fatigue strength.

Table 20. Results of Fatigue Strength Analysis for Validation.

Case	Numerical Fatigue Stress (MPa)	Result
1	375.412	Safe
2	371.526	Safe
3	411.297	Safe
4	431.808	Safe
5	425.408	Safe
6	449.725	Safe

The structural strength analysis was performed using geometric and material nonlinear analysis to evaluate whether the collapse strength of the structure exceeded the design pressure. As shown in Table 21, the results indicated that the collapse strength was 1.05 to 1.12 times greater than the design pressure for all cases, confirming sufficient structural strength. This verifies that the deep frames designed using the proposed initial scantling formulas are appropriate in terms of structural strength.

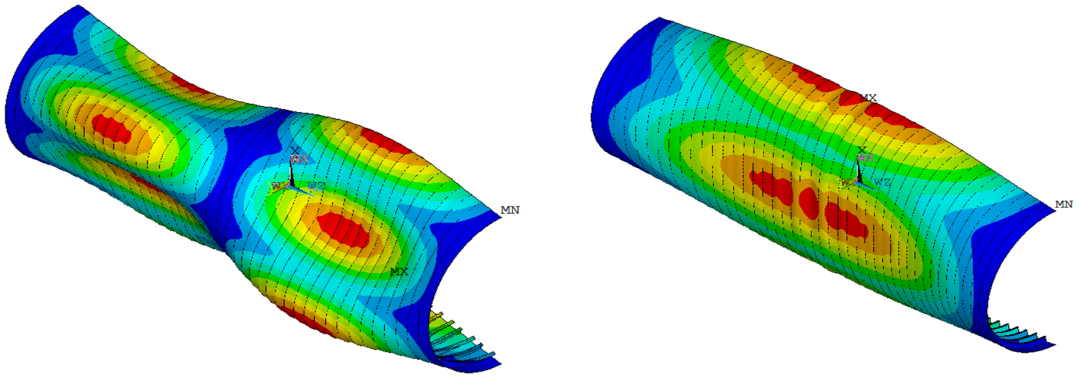
Table 21. Comparison of Design Pressure and Collapse Pressure for Structural Strength.

Case	1	2	3	4	5	6
P_{Design} (MPa)	5.500	6.000	5.50	6.000	7.000	7.500
P_{cr} (MPa)	6.175	6.325	6.175	6.725	7.450	8.100
P_{cr}/P_{Design} Ratio	1.12	1.05	1.12	1.12	1.06	1.08

The results of the linear analysis for general instability revealed two distinct buckling modes in all cases, as illustrated in Figures 10–15. As summarized in Table 22, the buckling mode in which the deep frame behaves as a bulkhead occurred prior to the mode where the deep frame deforms together with the shell. The latter mode does not enable the deep frame to perform its intended bulkhead function and is therefore structurally unfavorable if it occurs first. Therefore, to further verify the structural safety against buckling, a nonlinear analysis incorporating initial imperfections was performed for the buckling mode in which the deep frame acts as a transverse bulkhead. The results of the subsequent nonlinear analysis with initial imperfection, shown in Table 23, confirmed that the pressure hull and deep frame structures designed using the proposed formulas satisfy the design pressure under general instability conditions.

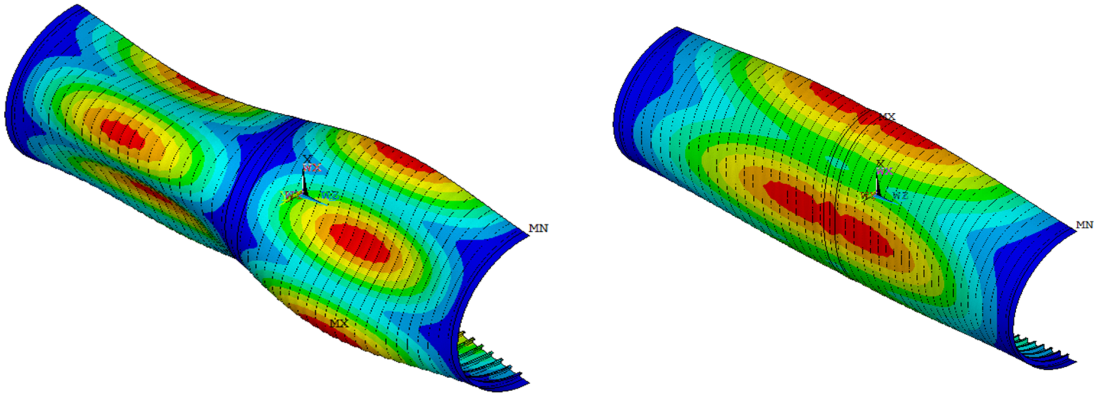
Table 22. Results of Linear Buckling Analysis for Validation.

Case	Mode No.	P_{cr} (MPa)	Case	Mode No.	P_{cr} (MPa)
1	54	20.85	4	15	23.78
	58	20.89		34	24.30
2	1	14.82	5	1	20.25
	2	15.00		2	20.39
3	1	19.46	6	5	24.30
	3	20.03		14	24.52



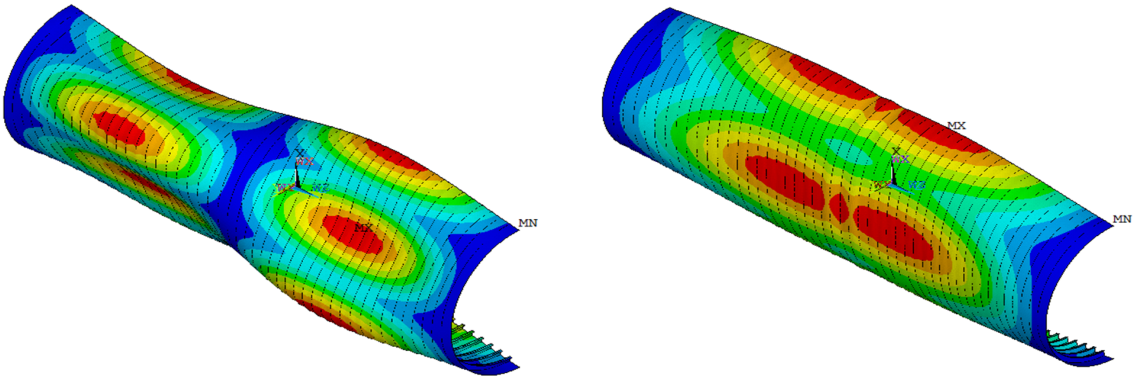
(**a**) Mode No.54 (**b**) Mode No.58

Figure 10. Linear Buckling Analysis Results for Case 1.



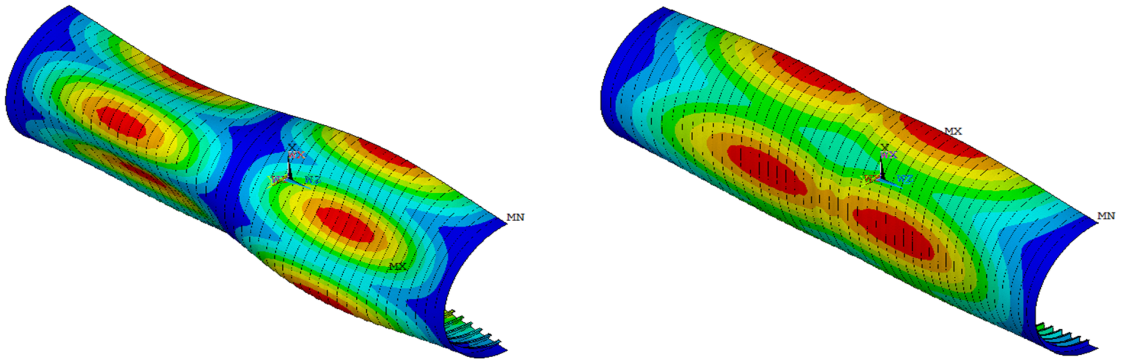
(**a**) Mode No.1 (**b**) Mode No.2

Figure 11. Linear Buckling Analysis Results for Case 2.



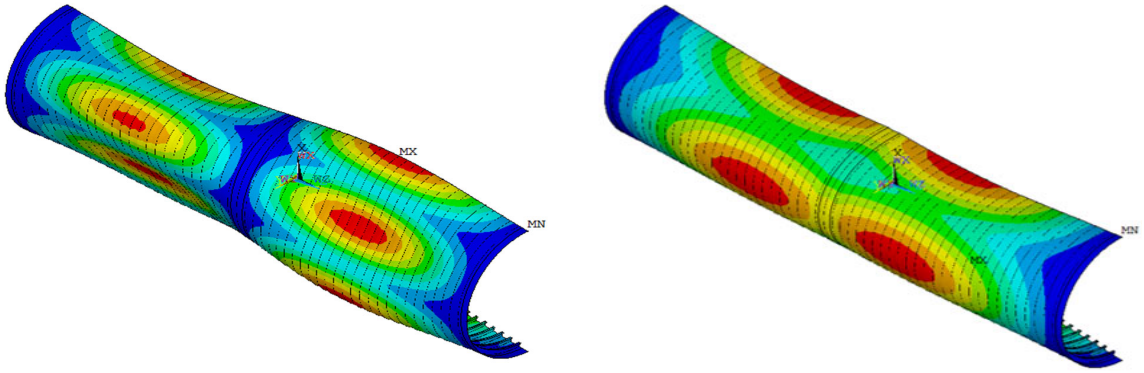
(**a**) Mode No.1 (**b**) Mode No.3

Figure 12. Linear Buckling Analysis Results for Case 3.



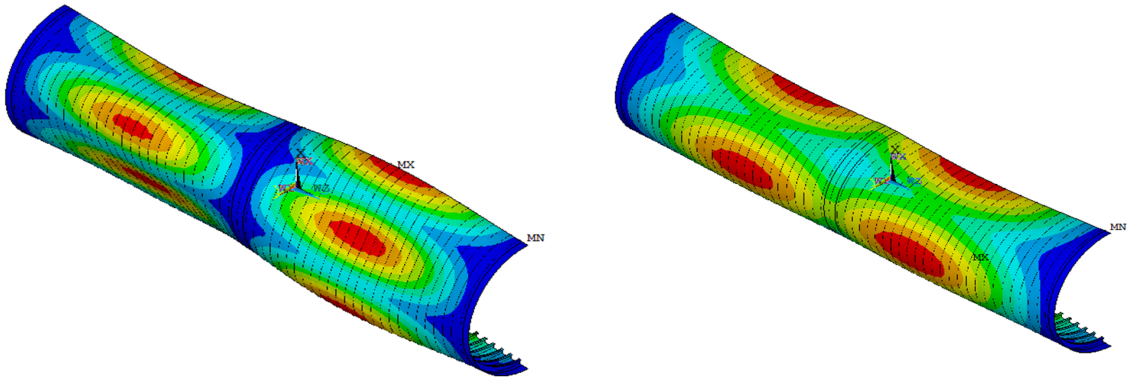
(**a**) Mode No.15 (**b**) Mode No.34

Figure 13. Linear Buckling Analysis Results for Case 4.



(**a**) Mode No.1 (**b**) Mode No.2

Figure 14. Linear Buckling Analysis Results for Case 5.



(**a**) Mode No.5 (**b**) Mode No.14

Figure 15. Linear Buckling Analysis Results for Case 6.

Table 23. Comparison of Design Pressure and Collapse Pressure for General Instability.

Case	1	2	3	4	5	6
P_{Design} (MPa)	5.500	6.000	5.50	6.000	7.000	7.500
P_{cr} (MPa)	6.100	6.275	6.100	6.680	7.500	8.100
P_{cr}/P_{Design} Ratio	1.11	1.03	1.11	1.11	1.07	1.07

8. Conclusions

In this study, six design cases with varying design pressures and pressure hull diameters were selected, and the corresponding ring frame dimensions were determined. The

structural safety of each case was verified through analyses of shell yielding (axisymmetric buckling), shell buckling (asymmetric buckling), and general instability. Based on these results, a total of 82,440 parametric studies were conducted for a section length range of $1.5\ D \leq L_{sec} \leq 2.0\ D$, using the following design variables: pressure hull section length (L_{sec}), reinforced shell thickness (t_{rein}), effective length (L_{eff}), web height (h_{wd}) and thickness (t_{wd}), and flange width (b_{fd}) and thickness (t_{fd}) of the deep frames. The initial scantling formulas for the deep frame dimensions were derived accordingly, as summarized in Table 17. The validity of the proposed formulas was then confirmed by conducting Validation analyses on selected cases, which demonstrated structural safety in terms of fatigue strength, structural strength, and general instability.

Author Contributions: Conceptualization, D.O.; Methodology, D.O.; Software, M.L. and D.O.; Validation, M.L. and D.O.; Formal analysis, M.L.; Investigation, M.L.; Resources, D.O.; Data curation, M.L.; Writing—original draft, M.L.; Writing—review and editing, D.O.; Visualization, M.L.; Supervision, D.O.; Project administration, D.O.; Funding acquisition, D.O. All authors have read and agreed to the published version of the manuscript.

Funding: This work was supported by the Hongik University new faculty research support fund.

Institutional Review Board Statement: Not applicable.

Informed Consent Statement: Not applicable.

Data Availability Statement: The data presented in this study are available on request from the corresponding author.

Acknowledgments: In this paper, ChatGPT-5.2 was used solely for English translation and minor sentence expression refinement. Its use was strictly limited to language-related assistance, and it was not used for generating or modifying the scientific content of the manuscript.

Conflicts of Interest: Author Minwoo Lee was employed by the company Naval Ship Design Department, Hanwha Ocean Co., Ltd. The remaining authors declare that the research was conducted in the absence of any commercial or financial relationships that could be construed as a potential conflict of interest.

References

1. Von Sanden, K.; Gunther, K. *The Strength of Cylindrical Shells, Stiffened by Frames and Bulkheads, Under Uniform External Pressure on All Sides*; David Taylor Model Basin: Carderock, MD, USA, 1952.
2. Faulkner, D. The Collapse Strength and Design of Submarines, RINA Symposium on Naval Submarine. 1983. Available online: https://www.scribd.com/document/437158582/Falkner-collapse-Strength-and-Design-of-Submarine-by-d-Falkner (accessed on 5 May 2025).
3. Lunchick, M.E. *Plastic Axisymmetric Buckling of Ring-Stiffened Cylindrical Shells Fabricated from Strain-Hardening Materials and Subjected to External Hydrostatic Pressure*; Report No. 1393; David Taylor Model Basin: Carderock, MD, USA, 1961.
4. Bryan, G.H. Application of the Energy Test to the Collapse of a Long Thin Pipe under External Pressure. In *Proceedings of the Cambridge Philosophical Society*; Cambridge University Press: Cambridge, UK, 1888; Volume 6, pp. 287–292. Available online: https://books.google.co.kr/books?id=zGlNC3UrYfsC&pg=PR3&hl=ko&source=gbs_selected_pages&cad=1#v=onepage&q&f=true (accessed on 5 May 2025).
5. Von Mises, R. Der Kritische Aussendruck für Allseits Belastete Zylindrische Rohre. In *Festschrift: Prof. Dr. A. Stodola zum 70. Geburtstag*; Orell Füssli: Zürich, Switzerland, 1929; pp. 418–430. Available online: https://archive.org/details/criticalexternal01vonm/mode/2up (accessed on 5 May 2025).
6. Windenburg, D.F.; Trilling, C. *Collapse by Instability of Thin Cylindrical Shells Under External Pressure*; Report No. 385; United States Experimental Model Basin: Washington, DC, USA, 1934.
7. Bryant, A.R. *Hydrostatic Pressure Buckling of a Ring-Stiffened Tube*; Report No. 306; NCRE: London, UK, 1954.
8. Kendrick, S. *The Buckling Under External Pressure of Circular Cylindrical Shells with Evenly Spaced, Equal Strength, Circular Ring-Frames: Part III*; NCRE Report No. R244; National Committee on Research in Engineering: London, UK, 1953.
9. Van der Neut, A. A General Solution of the Buckling of Spherical Shells, Considering Also Unsymmetric Buckling. Ph.D. Thesis, Delft University of Technology, Delft, The Netherlands, 1932.

10. Ross, C.T.F. *Pressure Vessels: External Pressure Technology*, 2nd ed.; Woodhead Publishing: Philadelphia, PA, USA, 2011.
11. Oh, D.; Koo, B. Empirical Initial Scantling Equations on Optimal Structural Design of Submarine Pressure Hull. *J. Adv. Res. Ocean Eng.* **2018**, *4*, 7–15.
12. Kine, H. Collapse Design Optimization of Ring-Stiffened Cylindrical Pressure Hulls. Master's Thesis, University of Stavanger, Stavanger, Norway, 2020.
13. Rathinam, N.; Prabu, B.; Anbazhaghan, N. Buckling analysis of ring stiffened thin cylindrical shell under external pressure. *J. Ocean Eng.* **2021**, *6*, 360–366. [CrossRef]
14. Serkan, Ş. A Structural Design Approach for Submarine Resistant Hull and Structural Optimization Based on Finite Element Method. Master's Thesis, ITU Institute of Science and Technology, İstanbul, Türkiye, 2021.
15. Thiago Kenji Leão, S.; Theodoro Antoun, N. Structural Optimization Applied to Submarine Pressure Hulls. *J. Ocean. Eng. Mar. Energy* **2025**, *11*, 169–182. [CrossRef]
16. Eyiler, B.; Bayraktarkatal, E. Investigation of Optimum Structures at Submarine Pressure Hulls under Hydrostatic Pressure with Finite Element Method. *J. Nav. Archit. Mar. Technol.* **2024**, *2024*, 25–35. [CrossRef]
17. Lee, J. *Ship and Offshore Structures*; Sejong Publishing: Seoul, Republic of Korea, 1996. (In Korean)
18. DNV, AS. *Rules for Classification—Naval Vessels: Part 8 Submarines*; Chapter 2, Structure; DNV: Høvik, Norway, 2024.
19. *MIL-S-16216K*; Military Specification: Steel Plate, Alloy, Structural, High Yield Strength. United States Department of Defense: Washington, DC, USA, 1987.
20. Pulos, J.G. *Structural Analysis and Design Considerations for Cylindrical Pressure Hulls*; Report No. 1639; The David Taylor Model Basin: Carderock, MD, USA, 1963.
21. Oh, D.; Ahn, N. Review of the Structural Shape for Aft Transition Ring of Submarine. *J. Korean Soc. Mar. Environ. Saf.* **2019**, *25*, 936–944. [CrossRef]

Disclaimer/Publisher's Note: The statements, opinions and data contained in all publications are solely those of the individual author(s) and contributor(s) and not of MDPI and/or the editor(s). MDPI and/or the editor(s) disclaim responsibility for any injury to people or property resulting from any ideas, methods, instructions or products referred to in the content.